

On numerical evincement of central limit theorem atypical behaviour in the Casati-Prosen triangle map

Sílvio M. Duarte Queirós¹

*Centro Brasileiro de Pesquisas Físicas, Rua Dr. Xavier Sigaud, 150,
22290-180 Rio de Janeiro-RJ, Brazil*

and

*Unilever R&D Port Sunlight, Quarry Road East, Wirral, CH63 3JW United
Kingdom*²

(9th December 2018)

Abstract

In this manuscript we analyse the behaviour of the probability density function of the sum of N deterministic variables generated from the triangle map. For the case in which the map is both ergodic and mixing the resulting probability density function quickly concurs with the Normal distribution. However, when the map is weakly chaotic, and apparently no mixing, the resulting probability density functions are described by power-laws with N dependent exponents smaller than 3 which become smaller as N increases. This power-law behaviour represents a clear departure from standard central limit theorem.

1 Introduction

The central limit theorem (CLT) has been subject of study within natural sciences for plenty of generations. As a matter of fact, we might state that CLT has originated in 1713 with Bernoulli's weak law of large numbers [1]. After him, de Moivre [2], Laplace [3], and Gauss, among others, made crucial contributions to the establishment of the Normal probability density function (PDF) as the stable distribution when one considers the sum of independent and identically distributed random variables with finite standard deviation. Nonetheless, the stability of the Normal distribution was just formally established by Russian mathematician Lyapunov 188 years after Bernoulli [4]. Afterwards, it was introduced the generalisation of CLT to independent and identically distributed random variables, but with infinite standard deviation by Lévy and Gnedenko [5, 6], followed by more sweeping generalisations which include dependency between variables [7, 8]. With the advent of computation in the 1970s, chaos theory and non-linear phenomena achieved huge progress. It was then possible to verify the existence of CLT for deterministic variables as well [9, 10]. More recently, CLT has been the focus of renewed interest within statistical mechanics mostly because of the endeavour to establish the optimising PDF of Tsallis non-additive entropy [11] as the stable distribution for the sum of random or

¹email address: Silvio.Queiros@unilever.com, sdqueiro@googlemail.com

²Present address

deterministic variables upon either some special kind of correlation [12] or on the edge of chaos [13] or even at a metastable state [14].

In the sequel of this manuscript we communicate results on numerical investigations of the distribution of deterministic variables which arise from the sum of variables generated from the triangle map introduced by Casati and Prosen in Ref. [15]. Our analysis is performed in two different regimes: a first one, for which the system is both *ergodic* and *mixing*, and a second in which the system is *weakly ergodic* and apparently *not mixing*. If in the former the convergence towards the Gaussian distribution is clear and easily explained according to standard CLT, for the latter case we detect an anomalous behaviour characterised by power-law PDF which diverts from the Gaussian distribution as the number of variables added increases. Such behaviour is unexpected along the lines of standard CLT. The manuscript is organised as follows: in Sec. 2 we introduce the triangular map and some of its properties, and in Sec. 3 we present our numerical results. Last of all, we reiterate some conclusions and remarks to Sec. 4.

2 The triangle map

The triangle map, $z_{t+1} = T(z_t)$ introduced by Casati and Prosen [15], corresponds to a discrete transformation on a torus $z = (x, y) \in [-1, 1) \times [-1, 1)$ with symmetrical coordinates,

$$\begin{cases} x_{n+1} &= x_n + y_n \pmod{2} \\ y_{n+1} &= y_n + \alpha \operatorname{sign} x_n + \beta \pmod{2} \end{cases}, \quad (1)$$

where $\operatorname{sign} x = \pm 1$, mod is the modulus function, and α and β are real parameters of the map. This map has emerged from studies on the compatibility between linear dynamical instability and the exponential decay of Poincaré recurrences. Map (1) is parabolic and area preserving. For the Jacobian matrix we have, $\det J = 1$, and its trace, $\operatorname{Tr} J = 2$.

Concerning the relevance of parameters α and β , it is known that when both of the parameters are irrational numbers, the map is ergodic [15]. Moreover, it attains the ergodicity property, *i.e.*, averages over time equal averages over samples, very rapidly. For such a set of values the map is also *mixing* in the sense that it has a *continuous spectral density*. Evaluating the Poincaré recurrences, it has been found that the probability of an orbit to stay outside a specific subset of the torus for a time longer than t goes as $\exp[-\mu t]$, with μ very close to the Lebesgue measure of the subset, fact that is in accordance with a completely stochastic dynamics. This decay leads to a linear separation of close orbits which has been related to non-extensive statistical mechanics formalism via a generalised Pesin-like identity that bridges the q -generalisation of Kolmogorov-Sinai entropy [16] and the q -Lyapunov coefficient from the sensitivity to initial conditions [17]. The entropic index for this map has been found to be $q = 0$ [18].

When $\alpha = 0$ and β is irrational the map is still ergodic [19], but is never mixing [20]. For the case $\beta = 0$ two situations might occur [15]. If α is a

rational number, then the dynamics is pseudo-integrable and confined, whereas for α being a irrational, the dynamics is found weakly ergodic, with the number of y_n taken form a single orbit increasing as $\ln T$ ($0 \leq n < T$). Furthermore, the ultra-slow apparent decay of the correlation function measured upon this condition does not provide sufficient evidence of mixing.

3 Results

In this section we present the numerical results from our analysis. Namely, we have considered variables X_N and Y_N that are obtained from the addition of x and y variables of map (1),

$$X_N = \sum_{i=1}^N x_i, \quad (2)$$

$$Y_N = \sum_{i=1}^N y_i. \quad (3)$$

We have neglected the $\alpha = 0$ case since it destroys the dependence of y on x and we have focussed on the following situations,

$$\text{case I : } \left\{ \alpha = \frac{1}{2} \left[\frac{1}{2} (\sqrt{5} - 1) - e^{-1} \right], \beta = \frac{1}{2} \left[\frac{1}{2} (\sqrt{5} - 1) + e^{-1} \right] \right\},$$

which corresponds to the ergodic and mixing case studied in Refs. [15, 18] and

$$\text{case II : } \left\{ \alpha = \pi^{-\frac{1}{2}}, \beta = 0 \right\},$$

where the map is weakly ergodic. For each analysis, we have randomly placed a set of initial conditions \mathcal{I} (typically 10^7 elements) within the torus z and we have let the map run. The probability density functions $P(X_N)$ and $P(Y_N)$ are then obtained from these \mathcal{I} initial conditions. Our numerical calculations have been performed using MATHEMATICATM kernel which assures great precision owe to its symbolic computation procedure.

For case I, as it is expected from ergodic and mixing properties of map (1) upon such conditions, both (detrended) X_N and Y_N approach the Normal distribution [10],

$$G(u_N) = \frac{1}{\sqrt{2\pi\sigma_N^2}} \exp \left[-\frac{1}{2\sigma_N^2} u_N^2 \right], \quad (4)$$

as N goes to infinity, see Fig. 1. In Eq. (4) u represents either X or Y , and σ_N is the standard deviation, $\sigma_N^2 = \frac{1}{N} \sum_{i=1}^N u_i^2$. Moreover, as it occurs in Lyapunov CLT, σ_N follows the scaling relation,

$$\sigma_N = \sqrt{N}\sigma_1,$$

Table 1: Values of the maximum value of $P(X_N)_{\max}$, and PDF exponent for positive, η_+ , and negative, η_- , branches for each value of N calculated.

N	$P(X_N)_{\max}$	η_+	η_-
10	0.350		
10^2	0.203	1.80	1.81
10^3	0.141	1.57	1.57
2×10^3	0.128	1.52	1.52
4×10^3	0.118	1.47	1.47
8×10^3	0.109	1.41	1.41
1.6×10^4	0.101	1.30	1.29

which is depicted in Fig. 2. In Ref. [15] a similar kind of analysis has been made by considering a cylinder $y \in (-\infty, \infty)$

$$y_n = y_0 + \beta n + \alpha p_n, \quad (5)$$

with $p_n \in \mathbb{Z}$.

We have also verified a skew on our PDFs, for small N , which are not visible on the PDFs of Ref. [15], but might be comprehended according to analytical work made on other types of maps by Beck and Roepstorff [9].

A completely dispair behaviour is found when case II is analysed. For this case we have concentrated on X_N , although for Y_N we have obtained the same qualitative results. Instead of a Normal distribution, we have numerically observed an asymptotic power-law decay for the respective probability density function,

$$P(u) \sim |u|^{-\eta-1}, \quad (6)$$

with an exponent $\eta < 2$ for every value of N analysed, see Tab. 1 and Figs. 3 and 4. The method applied to determine η has been the Meerschärt-Scheffler estimator (see Appendix) [21] which has proved to be more reliable than the Hill estimator. In spite the maxima of $P(X_N)$ are different from zero, we have verified that distributions have got the same decay exponent for both sides (within numerical error).

The upper bound of η imposes that the standard deviation is incommensurable if the variable is defined over the whole interval of real numbers. Since we are treating cases for which N is finite, the support of the resulting PDFs is compact and defined between $-N$ and N for X_N and Y_N . This leads to a finite standard deviation, σ_N , for the cases we have studied. We have verified that σ_N scaling its nearly described by a power-law with exponent 0.94 ± 0.02 , although it is visible that points are not fully aligned according to a straight line when depicted in log-log scale as we show in Fig 5. Additionally, and in opposition to what happens with the Lévy-Gnedenko generalisation of CLT, η is N dependent and decreases as N increases. Rigorously, we cannot consider this case as a deterministic analogue for Lévy-Gnedenko CLT simply because

the variables x_n and y_n are both restricted to interval $[-1, 1)$, hence having finite standard deviation, $\sigma_1 = \frac{1}{\sqrt{3}}$. The emergence of an inflexion point when we have plotted $P(X_N)$ in a log – log scale could sign the α -stable (or Lévy) ³,

$$\mathcal{L}_\alpha(X_N) = \frac{1}{2\pi} \int_{-\infty}^{+\infty} \exp[-i k X_N - a |k|^\alpha] dk, \quad (0 < \alpha < 2), \quad (7)$$

or similar distribution as the stable distribution for this problem. Nevertheless, if null hypothesis,

$$P(X_N) = \mathcal{L}_\alpha(X_N), \quad (N \rightarrow \infty),$$

should be verified, taking into account Lévy-Gnedenko CLT, we still cannot consider $\mathcal{L}_\alpha(X_N)$ as strictly stable since the exponent characterising the asymptotic limit $X_N \rightarrow \infty$ varies with N . This represents a quite interesting feature of this system.

Furthermore, when we try to infer on the scaling behaviour of $P(X_N)_{\max}$ with N , just like it has happened with σ_N , a clear-cut power-law behaviour could not be found as it is visible in Fig. 6.

4 Final remarks

In this manuscript we have presented a numerical study on the addition of deterministic variables generated by a conservative map, the triangle map of Casati and Prosen [15]. The study has been performed in two different regimes, case I and case II, by iterating the map from a set of initial conditions which have uniformly been distributed within interval $[-1, 1)$. In case I, for which the map is ergodic and mixing, the outcoming stable PDF is the Normal distribution for both X_N and Y_N , in perfect accordance with standard theory. In case II, for which the map is weakly ergodic and apparently no mixing, we have obtained PDFs which present asymptotic power-law behaviour. Moreover, the exponents obtained are N dependent and smaller than 3, the lower bound for finite second order moment of distributions defined between $-\infty$ and ∞ . This result is quite dazzling seeing that, notwithstanding the map is weakly ergodic, it fulfils the phase space as time evolves. Accordingly, it would be expected an approach to Gaussian behaviour. In such scenario the map would present some anomalous (quasi-steady) behaviour before total occupancy of phase space and then a crossover to the Normal distribution, like it has analogously been observed for the fractal dimension of low-dimensional symplectic maps (see details in Ref. [22]). However, the observed increasing departure from the Gaussian distribution as N increases points out into another direction⁴. Moreover, in our results the mixing property looks to be a crucial element, providing thus a corroboration of hierarchy mixing-ergodicity. It is worth to remember that in case II mixing has not been proved as well as the fact that the mixing property

³Here α is the exponent of the distribution and not the parameter of map (1).

⁴ N can also work as a measure of time.

is stronger than ergodicity [23]. Further analysis either considering larger values of N or along the lines of Ref. [9] might bring a clear picture of this interesting anomalous behaviour.

Acknowledgements

SMDQ would like to thank several discussions over several aspects of CLT with C. Tsallis and G. Ruiz for conversations about its application to deterministic variables. EP Borges, DO Soares-Pinto and PB Warren are acknowledged for the critical reading of the manuscript. The work herein presented benefited from financial support by FCT/MCTES (Portuguese agency) and Marie Curie Fellowship Programme (European Union), and infrastructural support from PRONEX/CNPq (Brazilian agency).

Appendix

It is well-known, at least within the statistical community, that the widely used Hill estimator [24] presents problems namely when applied to stable data [25]. The method introduced by Meerschaert and Scheffler [21] is based on the asymptotic limit of the sum of the variables of dataset $\{X_N\}$ under scrutiny. For heavy tail data these asymptotics depend only on the tail index of the probability density function, and not on the exact form of the distribution. Hence, if \mathcal{I} elements of a dataset are identically and (in)dependently distributed, and in addition its probability density function presents an asymptotic behaviour,

$$P(X_N) \sim |X_N|^{-\eta-1}, \quad (|X_N| \rightarrow \infty),$$

it can be proved (Theorem 1 in Ref. [21]) that,

$$\frac{1}{\eta} = \frac{\ln_+ \left[\sum_{i=1}^{\mathcal{I}} (X_{N,i} - \langle X \rangle)^2 \right]}{2 \ln \mathcal{I}}, \quad (\text{A1})$$

where $\langle X \rangle$ is the simple average $\langle X \rangle = \mathcal{I}^{-1} \sum_{i=1}^{\mathcal{I}} X_{N,i}$ and $\ln_+ [x] \equiv \max \{ \ln x, 0 \}$.

References

- [1] J. Bernoulli, *Ars Conjectandi* (Basel, 1713)
- [2] A. de Moivre, *The Doctrine of Chances* (Chelsea, New York, 1967)
- [3] P.-S. Laplace, *Théorie Analytique des Probabilités* (Dover, New York 1952)
- [4] A. M. Lyapunov, Bull. Acad. Sci. St. Petersburg **12** (8), 1 (1901)
- [5] P. Lévy, *Théorie de l'addition des variables aléatoires* (Gauthier-Villards, Paris, 1954)

- [6] B. V. Gnedenko, Usp. Mat. Nauk **10**, 115 (1944) (Translation nr. 45, Am. Math. Soc., Providence)
- [7] A. Araujo and E. Guiné, *The Central Limit Theorem for Real and Banach Valued Random Variables* (John Wiley & Sons, New York, 1980)
- [8] P. Hall and C. C. Heyde, *Martingale Limit Theory and Its Application* (Academic Press, New York, 1980)
- [9] C. Beck and G. Roepstorff, Physica A **145**, 1 (1987); C. Beck, J. Stat. Phys. **79**, 875 (1995)
- [10] M.C. Mackey and M. Tyran-Kaminska, Phys. Rep. **422**, 167 (2006)
- [11] C. Tsallis, J. Stat. Phys. **52**, 479 (1988)
- [12] L.G. Moyano, C. Tsallis and M. Gell-Mann, Europhys. Lett. **73**, 813 (2006); S. Umarov, C. Tsallis and S. Steinberg, arXiv:cond-mat/0603593 (pre-print, 2006); S. Umarov, C. Tsallis, M. Gell-Mann and S. Steinberg, arXiv:cond-mat/06006038 (pre-print, 2006); S. Umarov, C. Tsallis, M Gell-Mann and S. Steinberg, arXiv:cond-mat/06006040 (pre-print, 2006); S. Umarov, C. Tsallis, arXiv:cond-mat/0703533 (pre-print, 2007); F. Baldovin and A. Stella, Phys. Rev. E **75**, 020101(R) (2007); H.J. Hilhorst and G. Schehr, J. Stat. Mech. P06003 (2007)
- [13] U. Tirnakli, C. Beck and C. Tsallis, Phys. Rev. E **75**, 040106 (2007); G. Ruiz, S.M. Duarte Queirós and C. Tsallis (unpublished, 2007)
- [14] A. Pluchino, A. Rapisarda and C. Tsallis, EPL **80**, 26002 (2007)
- [15] G. Casati and T. Prosen, Phys. Rev. Lett. **85**, 4261 (2000)
- [16] F. Baldovin and A. Robledo, Phys. Rev. E **69**, 045202 (2004)
- [17] C. Tsallis, A.R. Plastino and W.-M. Zheng, Chaos, Solitons & Fractals **8**, 885 (1997)
- [18] G. Casati, C. Tsallis and F. Baldovin, Europhys. Lett. **72**, 355 (2005)
- [19] H. Furstenberg, Am. J. Math. **83**, 573 (1961)
- [20] I. P. Cornfeld, S.V. Fomin, and Ya.G. Sinai, *Ergodic Theory* (Springer-Verlag, New York, 1982).
- [21] M.M. Meerschaert and H.-P. Scheffer, J. Stat. Plan. Infer. **71**, 19 (1998)
- [22] F. Baldovin. E. Brigatti and C. Tsallis, Phys. Lett. A **320**, 254 (2004)
- [23] R. Kubo, H. Ichimura, N. Hatchisume, *Statistical Mechanics* (Norrholland, Amsterdam, 1988)
- [24] B. Hill, Ann. Statist. **3**, 1163 (1975)
- [25] J. McCulloch, J. Business Econ. Statist. **15**, 74 (1997)

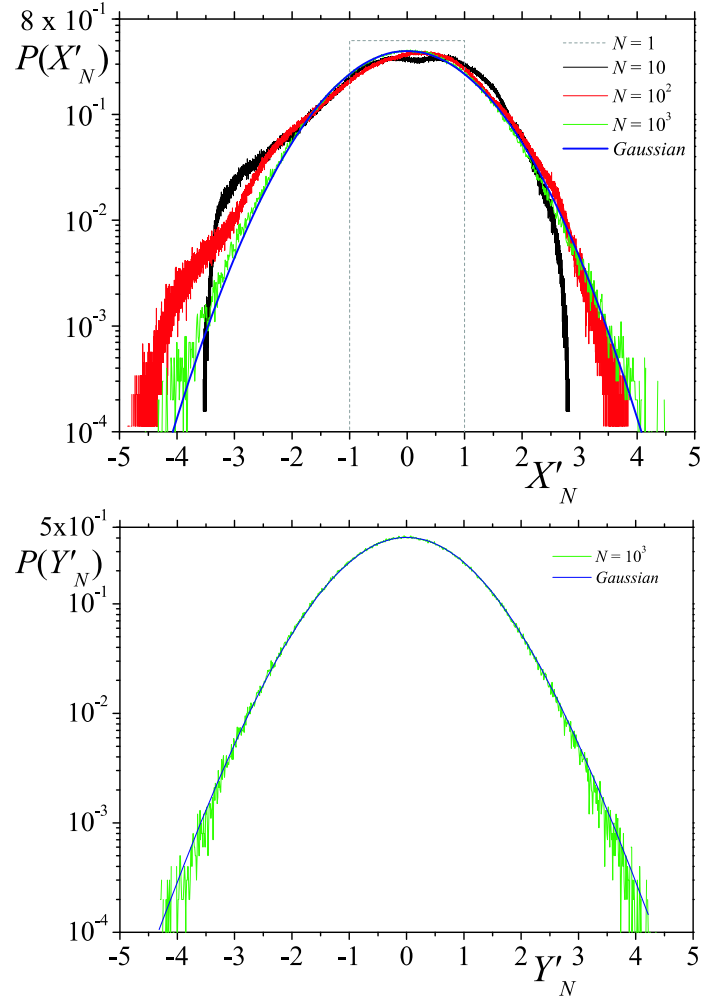


Figure 1: Upper panel: Probability density function $P(X'_N)$ vs. X'_N for scaled variables $X'_N \equiv X_N - \langle X_N \rangle / \sigma_N$, obtained in case I where $\langle X_N \rangle$ represents the average of X_N [in log-linear scale]. Lower panel: The same as the upper panel, but for variable Y_N . In both panels the line labelled *Gaussian* corresponds to Eq. (4) with $\sigma_N = 1$.

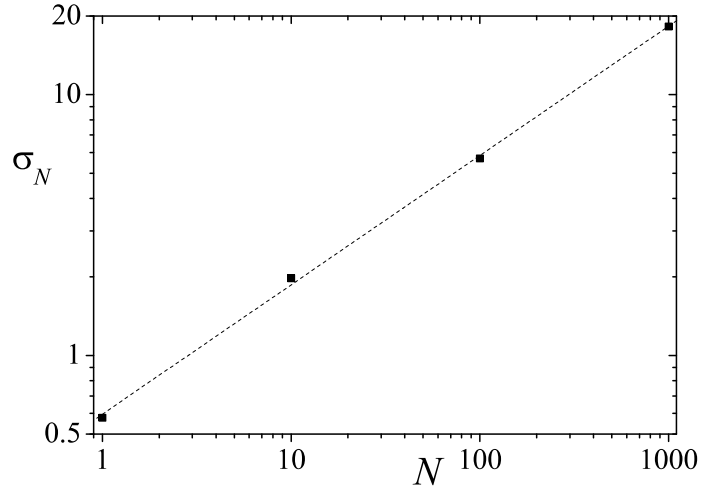


Figure 2: Standard deviation, σ_N , of X_N vs. N for case I [in log-log scale]. The fitting straight line has a slope of 0.49 ± 0.01 .

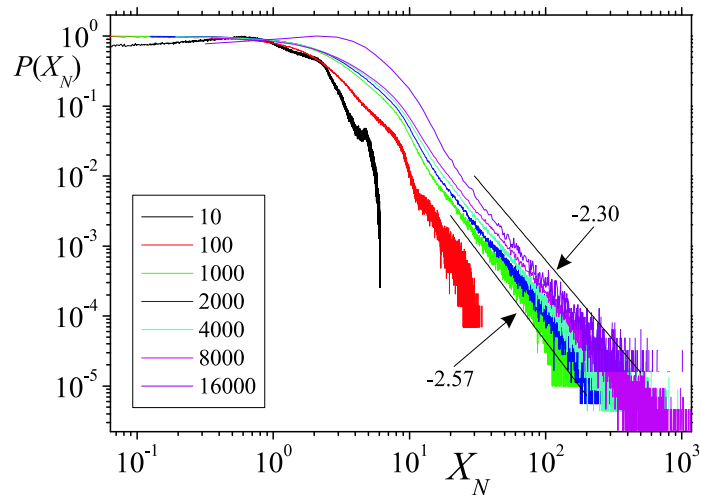


Figure 3: Probability density function $P'(X_N) = \frac{P(X_N)}{P(X_N)_{\max}}$ vs. X_N [in log-log scale]. The number of initial conditions (points used to construct PDFs) is 10^7 except for $N = 8000$ (7.5×10^6 points) and $N = 16000$ (7×10^5 points). The power-law decay is evident for large N . The two straight lines have slopes $-(\eta_+ + 1)$ with η the exponent for $N = 1000$ and $N = 16000$ (see Table 1).

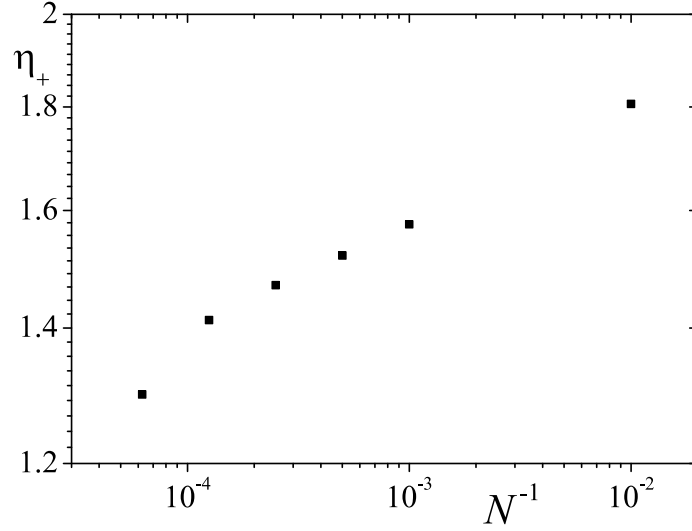


Figure 4: Values of the exponent for positive side, η_+ , vs. N^{-1} [in log-log scale].

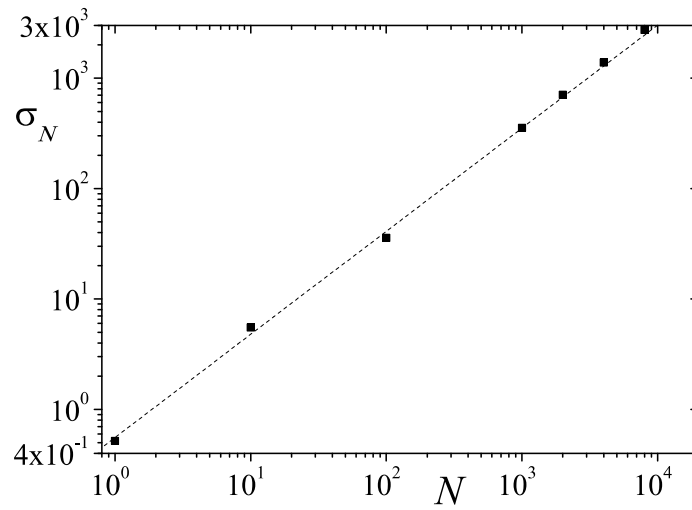


Figure 5: Standard deviation σ_N vs. N of X_N obtained from map (1) [in log-log scale]. The fitting dashed line has a slope 0.94 ± 0.02 ($R = 0.9995$).

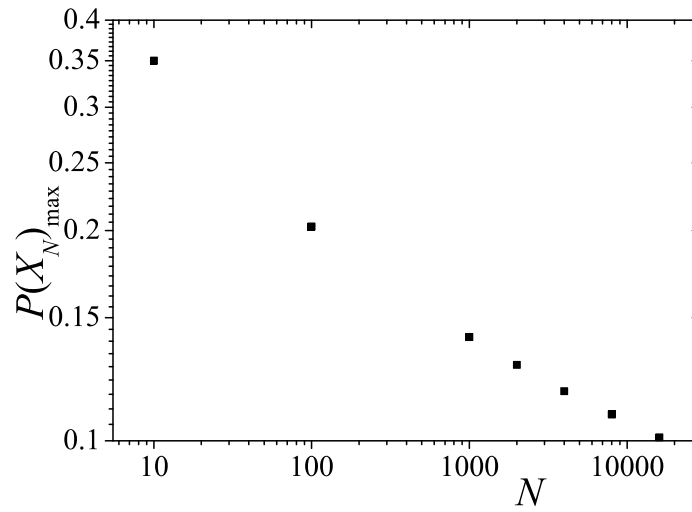


Figure 6: Maximum value $P(X_N)_{\max}$ vs. N according to the values of Table 1 [in log-log table].